ToGePi: Topology and Geometry informed Positional Information

Veljko Kovac, Gerard Planella, Adam Valin,
Luca Pantea

May 2023

1 Abstract

Graph neural networks (GNNs) have emerged as the dominant learning architectures for graph data. Among them, Equivariant Graph Neural Networks (EGNNs) introduced a novel approach to incorporate geometric information, ensuring equivariance throughout the system. However, the EGNN architecture has two main limitations. Firstly, it underutilizes the topological information inherent in the graph structure, and secondly, achieving SOTA performance necessitates a fully connected graph, which may not always be feasible in certain applications. In addition, the Learnable structural and Positional Encodings (LSPE) framework proposes to decouple structural and positional representations to learn better these two essential properties by using implicit topological information. In this work, we investigate the extent to which structural encodings in geometric methods contribute in capturing topological information. Furthermore, inspired by Equivariant Message Passing Simplicial Network (EMPSN) architecture, which integrates geometric and topological information on simplicial complexes, we introduce an approach that leverages geometry to enhance positional encodings within the LSPE framework. We empirically show through our proposed method that conditioning the learnable PEs with the absolute distance between particles (for the QM9 dataset) can be beneficial to learn better representations, given that the model has sufficient complexity. Our method exhibits promising potential for graph datasets with limited connectivity, offering opportunities for advantageous outcomes by effectively handling situations where achieving a fully connected graph is not feasible.

2 Introduction

Graph Neural Networks (GNNs), dating back to the 1990s, [Sperduti, 1993, Gori et al., 2005, Bruna et al., 2014, Kipf and Welling, 2016] have ascended from a niche of representation learning to one of its most successful methods. GNNs are commonly used for analyzing and processing graph data, as they have the capability to learn using local information and, to some extent, the global structural information of a graph. Their applications span a wide range of domains, from recommender systems [Ying et al., 2018] to drug discovery [Han et al., 2021].

A rather significant role in the success of GNNs is partially attributed to the message-passing

framework [Gilmer et al., 2017a], which enables nodes in a graph to exchange and aggregate information through iterative message passing steps, enhancing their representation and facilitating effective learning on graph-structured data. However, it has been shown that this framework suffers from fundamental limitations [Xu et al., 2018], which constrain their expressivity. More specifically, GNNs are shown to be as powerful as the 1-dimensional Weisfeiler-Lehman (WL) test [Weisfeiler and Leman, 1968] in distinguishing non-isomorphic (sub-)graphs [Morris et al., 2018]. Due to the locality of the message-passing framework, each node in GNNs only aggregates from its direct neighbours. This local view can be a drawback when trying to learn global graph properties or when the important features of a node are dependent on nodes beyond its immediate neighbourhood.

Recent research has been dedicated to enhancing the discriminative capabilities of GNNs, pushing past the constraints imposed by the 1-WL test. One solution to this issue involves providing inductive biases to the GNNs in the form of the data's geometric information [Satorras et al., 2021, Brandstetter et al., 2021]. While incorporating the distance norm improves the model's performance, it still suffers from limitations in expressivity by being unable to learn explicit higher-dimensional features in the graph. A different line of research focuses on providing this information through topology by integrating Positional Encodings (PE) such as Random Walk-based [Bourgain, 1985, Chung, 1997] or Laplacian Eigenvector-based Encodings [Dwivedi et al., 2022]. These techniques aim to capture more global information and provide a richer representation of the graph beyond immediate neighbourhood interactions. Another more recent approach involves using Learnable Structural and Positional Encodings (LSPE) [Dwivedi et al., 2021] to decouple the structural (node features) and positional (node's position within the graph) representations within GNNs, allowing them to be learned independently and leading to an increased expressivity and performance.

To further enhance the expressive power of GNNs, this research project takes inspiration from the Equivariant Message Passing Simplicial Network (EMPSN) architecture [Eijkelboom et al., 2023], a novel approach that combines geometric and topological information on simplicial complexes. Our goal is to develop a generic method that also combines geometric and topological information by improving upon the established LSPE framework. By combining these distinct approaches, we seek to leverage the complementary nature of geometric and topological information in capturing complex graph relationships and enhancing the discriminative capabilities of GNN models. We highlight the following contributions:

- By providing PE to geometric methods, we empirically find that topological information through structural encodings improves geometric methods in shallow models, while this effect diminishes as the models become deeper.
- We introduce a novel approach to incorporate geometric information into structural methods based on LSPE, which results in better-learnt representations, given that the model has sufficient complexity.

3 Related Works

3.1 Message Passing Neural Networks

Message Passing Neural Networks (MPNNs) have emerged as a popular class of models for graph representation learning. MPNNs allow nodes in a graph to exchange information with their neighbouring nodes through message-passing iterations, enabling the incorporation of local graph

structure into node representations. These models typically consist of two key steps: message propagation, where each node aggregates information from its neighbours, and node update, where the aggregated information is used to update the node's representation. MPNNs have demonstrated strong performance in various graph-related tasks, including node classification, link prediction, and graph generation. Several notable MPNN variants include Graph Convolutional Networks (GCNs) [Kipf and Welling, 2016], Graph Attention Networks (GATs) [Veličković et al., 2017], GraphSAGE [Hamilton et al., 2017] and Graph Isomorphism Networks (GIN) [Xu et al., 2018], each offering unique strategies for message passing and aggregation.

$$h_i^{\ell+1} = f_h\left(h_i^{\ell}, \left\{h_j^{\ell}\right\}_{j\in\mathcal{N}_i}, e_{ij}^{\ell}\right), h_i^{\ell+1}, h_i^{\ell} \in \mathbb{R}^d, \tag{1}$$

$$e_{ij}^{\ell+1} = f_e\left(h_i^{\ell}, h_j^{\ell}, e_{ij}^{\ell}\right), e_{ij}^{\ell+1}, e_{ij}^{\ell} \in \mathbb{R}^d \tag{2}$$

The generic MPNN framework equations are shown in Equations 1 and 2, where f_h and f_e are functions with learnable parameters, and $\mathcal{N}_i$ is the neighbourhood of the node i.

3.2 E(n) Equivariant GNN

EGNNs [Satorras et al., 2021] extend MPNNs by relying on graph geometry to improve performance and attain E(n) equivariance. One particular aspect that renders EGNNs highly effective in capturing graph-level topology yet computationally expensive is that they operate best in fully-connected settings with a moderately deep architecture. However, this approach might not always be feasible, as the number of layers needed to learn higher dimensional graph structures scales exponentially, which ultimately renders such architectures intractable for large graphs.

3.3 Positional Encodings

Positional encodings (PE) are a fundamental concept that significantly influences the effectiveness of many network architectures, including CNNs [Lecun et al., 1998], RNNs [Hopfield, 1982, Hochreiter and Schmidhuber, 1997], and most recently, Transformers [Vaswani et al., 2017], by providing a means to infuse positional information into deep learning models. However, inferring nodes' positions in any given graph is a non-trivial task due to the absence of a canonical positioning method for capturing both local and global information. While GNNs have been shown to outperform traditional algorithms for node classification, subpar performance was demonstrated in [Hu et al., 2020] when compared to simple heuristics such as Adamic Adar [Adamic and Adar, 2003] on link prediction tasks [Liben-Nowell and Kleinberg, 2003]. Recent work [Srinivasan and Ribeiro, 2019, Brüel-Gabrielsson et al., 2022, Wang et al., 2022] have (empirically) rendered the addition of PE in GNNs crucial in achieving state-of-the-art (SOTA) in graph prediction tasks. Several candidates for PE have been proposed, such as Index PE [Murphy et al., 2019], Laplacian Eigenvectors [Dwivedi et al., 2022] and learnable position-aware embeddings based on random anchor node sets [You et al., 2019]. Another relevant method which this study focuses on involves diffusion-based Random walks [Bourgain, 1985, Chung, 1997]. The encodings produced with this method carry significant descriptive power when considering graph topology, as they can effectively capture the graph's diffusion characteristics [Topping et al., 2022]. Formally, the RW matrix can be defined over k-steps as:

$$p_i^{\mathrm{RW}} = \left[\mathrm{RW}_{ii},\ \mathrm{RW}_{ii}^2,\ \ldots\ \mathrm{RW}_{ii}^k\right] \tag{3}$$

where $p_i^{\mathrm{RW}} \in \mathbb{R}^k$ is initial PE of node i, and $\mathrm{RW} = AD^{-1}$, given the adjacency matrix A and the degree matrix D. Moreover, the intuition behind RW_{ii}^k can be interpreted as the probability of starting and ending a k-hop random walk on node i. Appendix A presents a more detailed study of Random Walk PE.

3.4 Learnable Structural and Positional Encodings

Learnable Structural and Positional Encodings (LSPE) [Dwivedi et al., 2021] have been proposed as an extension to traditional GNN architectures. LSPE combines structural and positional encodings to learn expressive representations that better capture both local and global graph information, resulting in more expressive node embeddings. The structural encoding component focuses on connectivity patterns and neighbourhood information, while the positional encoding component provides topological information into the node representations.

Incorporating LSPE into GNNs enhances the GNN's capability to better capture both local and global graph characteristics, enabling better handling of complex graph structures. The learnable nature of the encodings allows the model to adapt and optimize representations for specific tasks, making it suitable for diverse graphs with varying structural and positional properties. The combination of structural and positional encodings provides a richer representation of the graph, manifested through more expressive node embeddings, leading to improved performance in node classification, link prediction, and graph generation tasks.

$$h_i^{\ell+1} = f_h\left(\begin{bmatrix} h_i^\ell \\ p_i^\ell \end{bmatrix}, \left\{\begin{bmatrix} h_j^\ell \\ p_j^\ell \end{bmatrix}\right\}_{j\in\mathcal{N}_i}, e_{ij}^\ell\right), h_i^{\ell+1}, h_i^\ell \in \mathbb{R}^d, \tag{4}$$

$$e_{ij}^{\ell+1} = f_e\left(h_i^\ell, h_j^\ell, e_{ij}^\ell\right), e_{ij}^{\ell+1}, e_{ij}^\ell \in \mathbb{R}^d \tag{5}$$

$$p_i^{\ell+1} = f_p\left(p_i^\ell, \left\{p_j^\ell\right\}_{j\in\mathcal{N}_i}, e_{ij}^\ell\right), p_i^{\ell+1}, p_i^\ell \in \mathbb{R}^d \tag{6}$$

As we observe in Equation 4, it becomes apparent that the only deviations from the original MPNN equations 1 and 2 are the addition of a positional representation update as seen in Equation 6 and the concatenation of these trainable PEs with the node structural features as seen in Equation 4.

3.5 Topological approaches

No explicit topological properties have been used in all the aforementioned techniques, where relational structure about the system in a higher dimensional space could be encoded. The Graph Substructure Network (GSN) [Bouritsas et al., 2022] is considered to be one of the earlier methods that incorporated topology into its architecture, which laid the foundation for many subsequent research papers on topological deep learning [Papillon et al., 2023]. GSN enhanced the message-passing scheme with structural features extracted by (sub-)graph isomorphism. Furthermore, a novel message-passing procedure was introduced [Bodnar et al., 2021] that focuses on the "lifting"

map of induced cycles within a graph. This enables the network to distinguish between rings within atoms on molecular datasets more easily, increasing its expressivity beyond that of the WL test. Finally, E(n) equivariant Message Passing Simplicial Networks [Eijkelboom et al., 2023] have combined geometric and topological graph approaches in their architecture. They re-formulated the original EGNN [Satorras et al., 2021] to enable learning of features on simplicial complexes. The approach involves lifting the map and including information about the relative positions of communicating simplices in the message-passing formulation, demonstrating the potential to obtain SOTA for approaches that combine topology and geometry.

4 Methodology

Recognizing the significant role of node distances in capturing the graph's topology within the original EGNN architecture and the promising results of the LSPE framework as mentioned in Subsection 3.4, we propose a method which combines these two techniques. By integrating the geometrical features of the graph (node distances in the case of QM9) with topological features given by PEs, we seek to achieve more expressive node attributes.

4.1 Topology and Geometry informed LSPE

As mentioned in Section 3, EGNNs have achieved remarkable success by using the underlying geometry of the graph space to their advantage. However, it is important to note that the computational cost associated with fully connected graphs can limit the feasibility of this approach. As the dimensionality of the graph structures increases (e.g. cycles), the number of layers required to learn such higher-dimensional structures scales exponentially. For that reason, we first aim to explore the benefits of incorporating implicit topology in the EGNN framework. This is performed by using a random walk encoding (k = 24), explained in Section 3.2, by embedding the hidden features of a node together with its positional encoding to a higher dimensional space through concatenation.

Our method proposes to combine the LSPE method while also making use of the geometrical information found in EGNNs, by taking relative absolute distances between nodes into account in the message function. The additional feature, the norm of distance in this case, is added through concatenation to the message network for both the node message and the PE message as can be seen in Table 1. One benefit of this method is that parameter count does not drastically increase when adding LSPE with Geometry as only one scalar attribute is added to each MPNN layer.

4.2 MPNN Variants

Two different MPNN architectures were examined in this study. The first one, which this study refers to as *Standard* MPNN, calculates the messages based on both receiving and sending nodes whereas the second architecture, the *Isotropic* MPNN [Tailor et al., 2022], only uses sending nodes to calculate messages, allowing us to test our method on less expressive models.

In order to quantify the contribution of geometry in the LSPE framework, we run a set of experiments on 6 variants. These include the basic MPNN model, adding Geometry only (for which the Standard MPNN with Geometry resembles the EGNN), PE only, PE and Geometry, LSPE and LSPE with Geometry. The last one being our proposal described in 4.1. For all the aforementioned models

Model Architecture		
Message	Standard	$m_{ij} = \phi_e(h_i^\ell, h_j^\ell)$
	Isotropic	$m_{ij} = \phi_e(h_j^\ell)$
Message Geom.	Standard	$m_{ij} = \phi_e(h_i^\ell, h_j^\ell, \|\|x_i^\ell - x_j^\ell\|\|^2)$
	Isotropic	$m_{ij} = \phi_e(h_j^\ell, \|\|x_i^\ell - x_j^\ell\|\|^2)$
Agg.		$m_i = \sum_{j \neq i} m_{ij}$
Update	PE_{init}.	$h_i^{\ell+1} = \phi_h(h_i^\ell, m_i)$ $h_i^{\ell=0} = \phi_{embed}(\left[\begin{smallmatrix} h_i^{in} \\ p_i^{in} \end{smallmatrix}\right])$
	No PE_{init}	$h_i^{\ell+1} = \phi_h(h_i^\ell, m_i)$ $h_i^{\ell=0} = \phi_{embed}(h_i^{in})$

Table 1: Equations for message passing, aggregation and node update for MPNN, MPNN-Geom(EGNN), MPNN-PE, MPNN-PE-Geom (EGNN with PE) for both standard and isotropic MPNNs.

including PEs, we used a Random Walk (RW) diffusion-based positional encoding scheme as described in Section 2.2. The detailed formulas for each model can be found in Tables 1 and 2.

5 Experiments

Data The QM9 dataset, first introduced by [Ramakrishnan et al., 2014] and subsequently studied by [Gilmer et al., 2017b] and [Wu et al., 2018], comprises approximately 130,000 graphs, each consisting of around 18 nodes. In this dataset, the graphs represent molecules, with the nodes representing atoms and the undirected, typed edges representing various types of bonds between these atoms. The objective of analyzing this dataset is to predict 13 quantum chemical properties. Nevertheless, this study only focuses on inferring the Isotropic Polarizability α.

Implementation Details Our experimental setting is comprised of two main sets of experiments, focusing on the architectures that are *Standard* MPNNs and *Isotropic* MPNNs. For each architecture, we tested 6 different variants that are mentioned in Section 4.2. All model equations are shown in Tables 1 and 2. The structure of the table aims to describe the three following MPNN components, namely i) messages ii) aggregation and iii) node update operations. For the first experiment, our EGNN network (MPNN-Geom) is configured with 1, 4, and 7 hidden layers, while for the second experiment, we used 4 and 7 layers for all the models. Moreover, for this second experiment, we also tested a 10-layer Isotropic MPNN. Each network has 128 features per hidden layer and uses the SiLU activation function [Elfwing et al., 2017] as a non-linearity, with the exception of networks related to PEs, which use Tanh as an activation function. The predicted value is obtained by

Model Architecture		
Message	Standard	$m_{ij}^h = \phi_e(\begin{bmatrix} h_i^\ell \\ p_i^\ell \end{bmatrix}, \begin{bmatrix} h_j^\ell \\ p_j^\ell \end{bmatrix})$
	Isotropic	$m_{ij}^h = \phi_e(\begin{bmatrix} h_j^\ell \\ p_j^\ell \end{bmatrix})$
Message Geom.	Standard	$m_{ij}^h = \phi_e(\begin{bmatrix} h_i^\ell \\ p_i^\ell \end{bmatrix}, \begin{bmatrix} h_j^\ell \\ p_j^\ell \end{bmatrix}, \|\|x_i^\ell - x_j^\ell\|\|^2)$
	Isotropic	$m_{ij}^h = \phi_e(\begin{bmatrix} h_j^\ell \\ p_j^\ell \end{bmatrix}, \|\|x_i^\ell - x_j^\ell\|\|^2)$
PE Message	Standard	$m_{ij}^p = \phi_{pe}(PE_i^\ell, PE_j^\ell)$
	Isotropic	$m_{ij}^p = \phi_{pe}(PE_j^\ell)$
PE Message Geom.	Standard	$m_{ij}^p = \phi_{pe}(PE_i^\ell, PE_j^\ell, \|\|x_i^\ell - x_j^\ell\|\|^2)$
	Isotropic	$m_{ij}^p = \phi_{pe}(PE_j^\ell, \|\|x_i^\ell - x_j^\ell\|\|^2)$
Agg.		$m_i = \sum_{j \neq i} m_{ij}$
Update	Hidden upd.	$h_i^{\ell+1} = \phi_h(h_i^\ell, m_i^h)$ $h_i^{\ell=0} = \phi_{embed}(h_i^{in})$
	PE upd.	$PE_i^{\ell+1} = \phi_p(PE_i^\ell, m_i^p)$ $PE_i^{\ell=0} = \phi_{pemb}(PE_i^{in})$

Table 2: Equations for message passing, aggregation, and node update for MPNN-LSPE and MPNN-LSPE-Geom for both standard and isotropic MPNNs.

applying a sum-pooling operation followed by two layers of MLPs, which map the node embeddings $h^{(l=L)}$ to the output of the model. All models have been trained under the same configuration, with a batch size of 96, 1000 epochs, the Adam optimizer with a learning rate set at 0.0005 with a Cosine Annealing scheduler [Loshchilov and Hutter, 2017] and a weight decay of 10^{-16}. Further implementation details can be found in the repository's[1] implementation of the different models.

6 Results and Analysis

In this section, we will first examine how infusing the models with implicit topological information in the shape of Random Walk PEs (RWPE) affects their performance on the QM9 dataset in a fully connected (FC) and non-fully connected (NFC) setting. Moreover, we will demonstrate how geometrical information, the absolute distance between nodes, can be utilized effectively to learn better node embeddings.

In our first experiment, as mentioned in Subsection 3.3, we evaluated the EGNN using both original edges, and fully connected ones, with and without infusing the Positional Encodings. When comparing the performance for the different kinds of connections between the nodes, it can be seen from Table 4, that **the performance when all the nodes are connected is better in all experiments**. One reason for this boost in performance could be attributed to the EGNN architecture using geometry to learn the important edges. Also, as expected, in all of our results, it can be seen that more layers result in a higher performance, which is explained by the fact that each layer can gradually gather and incorporate information from neighbouring nodes and edges, capturing information from different hops in the graph.

Furthermore, to examine the trade-off between model complexity and the contribution of the topological information when embedded together with the hidden state, different numbers of layers were used for evaluation. From Table 4, it can be observed that the effect of PEs becomes more pronounced with a lower number of layers in the EGNN, suggesting that PEs play a crucial role in compensating for the challenges faced by shallower models in capturing distant topological information within the graph structure. On the other hand, **as model complexity increases, the EGNN architecture does not particularly benefit from the use of PEs**, especially in the FC setting. One possible explanation for this effect is that the EGNN model is able to implicitly learn topology by using the graph's geometry. In addition, it is interesting to mention that the 1-layer EGNN with no PEs obtains a much better performance in a FC setting, which can be attributed to the fact that in the FC setting the EGNN can better capture long-range dependencies as the whole graph becomes accessible in one hop.

For the second experiment, we trained both model architectures and all of their variants on the QM9 dataset for 4 and 7 layers in a NFC setting. The results are shown in table 4. The MPNNs introduced in Section 4.1 were used for these experiments. When analysing the effect of adding PEs, the performance for both Standard and Isotropic MPNN models increases, while for 7 layers the performance gained from using PEs is lessened. This can be related to the results from the first experiment, where a trade-off between model complexity and the contribution of topological information is experienced. This might suggest that **the EGNN (MPNN-Geom) model uses geometry to learn topology**. As for the combination of PE and Geometry through stacking

[1] https://github.com/gerardPlanella/LSPE-EGNN

Number of layers	FC	PEinit	Test MAE
1 layer	×	×	0.318
	×	✓	0.273
	✓	×	0.158
	✓	✓	0.144
4 layers	×	×	0.284
	×	✓	0.237
	✓	×	0.126
	✓	✓	0.124
7 layers	×	×	0.251
	×	✓	0.230
	✓	×	0.113
	✓	✓	0.114

Table 3: EGNN: (MPNN Geom vs MPNN Geom PE) Analysis of the effect of non-learnable PEs on the original QM9 data versus the fully connected QM9 data for different numbers of layers.

(PE-Geom), we can observe how performance is always improved compared to only using PE with the 4-layer models. An interesting finding is that for the 7-layer models, performance gain actually increases with model complexity for the MPNN-Isotropic. This indicates that the trade-off point has not yet been reached and thus signifying that MPNN-Isotropic can utilize better the stacked PE with Geometry.

When analysing the results for the models using LSPE, they show that the normal MPNN model always results in an increased performance while the opposite happens for the Isotropic MPNN. We thus hypothesise that **the model is not complex enough to effectively use the learnt PEs**. For LSPE with Geometry, we again see a similar effect as previously mentioned, with MPNN-LSPE-Geom achieving consistently the best performance for 4 and 7 layers. For the Isotropic MPNN, we experience a performance gain with respect to the base model, but infusing PEs (PE-Geom) still results in a better performance. It is worth mentioning that the performance gap between PE-Geom and LSPE-Geom becomes smaller for the Isotropic model as the number of layers increases, which supports our previous claim, that more complexity is needed to use the learnable encodings efficiently.

Motivated by the previous findings, we also trained the MPNN-Isotropic architecture and its variants under the same conditions for 10 layers to examine whether our previous hypothesis will be supported. The results are shown in Table 5, where we can see how **the LSPE-Geom model outperforms both the PE and PE-Geom models**, and with the LSPE model resulting in the worst performance. This not only proves that more complexity was needed to better use the learnt encodings, but it also demonstrates how our method for integrating topology and geometry is applicable to different models, resulting in a better overall performance than just using LSPE without geometry.

Architecture	**Test MAE (4-L)**	**Test MAE (7-L)**
MPNN	0.274	0.245
MPNN-Geom	0.285	0.251
MPNN-PE	0.241	0.227
MPNN-PE-Geom	0.237	0.230
MPNN-LSPE	0.255	0.223
MPNN-LSPE-Geom	**0.227**	**0.216**
MPNN-Isotropic	0.270	0.245
MPNN-Isotropic-Geom	0.260	0.244
MPNN-Isotropic-PE	0.258	0.239
MPNN-Isotropic-PE-Geom	**0.254**	**0.225**
MPNN-Isotropic-LSPE	0.269	0.245
MPNN-Isotropic-LSPE-Geom	0.267	0.231

Table 4: Analysis of the effect of different variants of MPNN and MPNN-Isotropic architectures on Test MAE for 4 and 7 layers.

Architecture	**Test MAE (10-L)**
MPNN-Isotropic	0.232
MPNN-Isotropic-Geom	0.226
MPNN-Isotropic-PE	0.231
MPNN-Isotropic-PE-Geom	0.238
MPNN-Isotropic-LSPE	0.252
MPNN-Isotropic-LSPE-Geom	**0.219**

Table 5: Analysis of the effect of different variants of MPNN-Isotropic architectures on Test MAE for 10 layers.

7 Conclusion

This work examines how injecting topological information into the EGNN model affects its performance in a fully connected and non-fully connected setting. Through an extensive investigation, we compared the original architecture with an enhanced version incorporating additional implicit topological information via Random Walk Positional Encodings. Our experiments revealed how, depending on the model's size, using implicit topological information may be beneficial to the EGNN's performance. Notably, these benefits were particularly prominent when using fewer layers in the EGNN, effectively addressing the challenge of capturing distant topological information encountered by shallower models. Furthermore, as the model complexity increased, the contribution of topological information diminished, suggesting a trade-off between model complexity and the incorporation of implicit topological knowledge in the EGNN architecture.

Recognizing the value of additional topological information in enhancing structural representations and inspired from the benefits of EGNN and the LSPE method, this work proposes a generic approach to leverage geometry for improved positional encodings when utilizing LSPE. This method achieved the best performance when models have sufficient computational complexity to make use of this additional information indicating that geometry can be indeed utilized to learn better structural and positional encodings, thus obtaining better results.

While our empirical study shows promising results in combining geometry and topology, several limitations in our study could benefit from further research. Future investigations should involve conducting experiments with a wider range of GNN architectures to expand our understanding of their interaction with topological information. Regarding the dataset, trying our method on inferring more tasks of the QM9 dataset could be beneficial.

Using LSPE entails higher computational complexity, however, a proposition that could be further investigated is whether we can use less complex layers to learn the same PEs by applying geometry. This becomes particularly relevant as we observe the enhanced performance with increased layers. Moreover, our present method of conditioning, achieved exclusively through concatenation, could be extended to alternatives that could potentially offer more efficient or expressive results. Additionally, our methodology presents promising potential for application on datasets where topological information is valuable but it is computationally prohibitive to connect all nodes. Through the utilization of our approach, one could potentially achieve an equilibrium between computational feasibility and the use of topological information. Moreover, while the EGNN paper[Satorras et al., 2021] tests the model in the QM9 dataset with the nodes' coordinates fixed, one could evaluate the same framework on datasets which coordinates are updated in order to examine the way that topological information (PEs) interacts with the coordinate update. Finally, considering the exceptional performance of the EGNN framework in fully connected settings without the need for LSPE, we believe that our method holds promise when applied to graph datasets where the fully connected setting is computationally prohibitive, potentially leading to favourable outcomes.

References

[Adamic and Adar, 2003] Adamic, L. A. and Adar, E. (2003). Friends and neighbors on the web. *Social Networks*, 25(3):211–230.

[Bodnar et al., 2021] Bodnar, C., Frasca, F., Otter, N., Wang, Y., Lio, P., Montufar, G. F., and Bronstein, M. (2021). Weisfeiler and lehman go cellular: Cw networks. *Advances in Neural Information Processing Systems*, 34:2625–2640.

[Bourgain, 1985] Bourgain, J. (1985). On lipschitz embedding of finite metric spaces in hilbert space. *Israel Journal of Mathematics*, 52:46–52.

[Bouritsas et al., 2022] Bouritsas, G., Frasca, F., Zafeiriou, S., and Bronstein, M. M. (2022). Improving graph neural network expressivity via subgraph isomorphism counting. *IEEE Transactions on Pattern Analysis and Machine Intelligence*, 45(1):657–668.

[Brandstetter et al., 2021] Brandstetter, J., Hesselink, R., van der Pol, E., Bekkers, E. J., and Welling, M. (2021). Geometric and physical quantities improve e (3) equivariant message passing. *arXiv preprint arXiv:2110.02905*.

[Bruna et al., 2014] Bruna, J., Zaremba, W., Szlam, A., and Lecun, Y. (2014). Spectral networks and locally connected networks on graphs. In *International Conference on Learning Representations (ICLR2014), CBLS, April 2014*.

[Brüel-Gabrielsson et al., 2022] Brüel-Gabrielsson, R., Yurochkin, M., and Solomon, J. (2022). Rewiring with positional encodings for graph neural networks.

[Chung, 1997] Chung, F. R. K. (1997). *Spectral Graph Theory*. American Mathematical Society.

[Dwivedi et al., 2022] Dwivedi, V. P., Joshi, C. K., Luu, A. T., Laurent, T., Bengio, Y., and Bresson, X. (2022). Benchmarking graph neural networks.

[Dwivedi et al., 2021] Dwivedi, V. P., Luu, A. T., Laurent, T., Bengio, Y., and Bresson, X. (2021). Graph neural networks with learnable structural and positional representations. *arXiv preprint arXiv:2110.07875*.

[Eijkelboom et al., 2023] Eijkelboom, F., Hesselink, R., and Bekkers, E. (2023). E(n) equivariant message passing simplicial networks.

[Elfwing et al., 2017] Elfwing, S., Uchibe, E., and Doya, K. (2017). Sigmoid-weighted linear units for neural network function approximation in reinforcement learning.

[Gilmer et al., 2017a] Gilmer, J., Schoenholz, S. S., Riley, P. F., Vinyals, O., and Dahl, G. E. (2017a). Neural message passing for quantum chemistry. *CoRR*, abs/1704.01212.

[Gilmer et al., 2017b] Gilmer, J., Schoenholz, S. S., Riley, P. F., Vinyals, O., and Dahl, G. E. (2017b). Neural message passing for quantum chemistry. In Precup, D. and Teh, Y. W., editors, *Proceedings of the 34th International Conference on Machine Learning*, volume 70 of *Proceedings of Machine Learning Research*, pages 1263–1272. PMLR.

[Gori et al., 2005] Gori, M., Monfardini, G., and Scarselli, F. (2005). A new model for learning in graph domains. In *Proceedings. 2005 IEEE International Joint Conference on Neural Networks, 2005.*, volume 2, pages 729–734 vol. 2.

[Hamilton et al., 2017] Hamilton, W., Ying, Z., and Leskovec, J. (2017). Inductive representation learning on large graphs. *Advances in neural information processing systems*, 30.

[Han et al., 2021] Han, K., Lakshminarayanan, B., and Liu, J. Z. (2021). Reliable graph neural networks for drug discovery under distributional shift. *CoRR*, abs/2111.12951.

[Hochreiter and Schmidhuber, 1997] Hochreiter, S. and Schmidhuber, J. (1997). Long short-term memory. *Neural computation*, 9:1735–80.

[Hopfield, 1982] Hopfield, J. J. (1982). Neural networks and physical systems with emergent collective computational abilities. *Proceedings of the National Academy of Sciences*, 79(8):2554–2558.

[Hu et al., 2020] Hu, W., Fey, M., Zitnik, M., Dong, Y., Ren, H., Liu, B., Catasta, M., and Leskovec, J. (2020). Open graph benchmark: Datasets for machine learning on graphs. *CoRR*, abs/2005.00687.

[Kipf and Welling, 2016] Kipf, T. N. and Welling, M. (2016). Semi-supervised classification with graph convolutional networks. *CoRR*, abs/1609.02907.

[Lecun et al., 1998] Lecun, Y., Bottou, L., Bengio, Y., and Haffner, P. (1998). Gradient-based learning applied to document recognition. *Proceedings of the IEEE*, 86(11):2278–2324.

[Liben-Nowell and Kleinberg, 2003] Liben-Nowell, D. and Kleinberg, J. (2003). The link prediction problem for social networks. In *Proceedings of the Twelfth International Conference on Information and Knowledge Management*, CIKM '03, page 556–559, New York, NY, USA. Association for Computing Machinery.

[Loshchilov and Hutter, 2017] Loshchilov, I. and Hutter, F. (2017). Sgdr: Stochastic gradient descent with warm restarts.

[Morris et al., 2018] Morris, C., Ritzert, M., Fey, M., Hamilton, W. L., Lenssen, J. E., Rattan, G., and Grohe, M. (2018). Weisfeiler and leman go neural: Higher-order graph neural networks. *CoRR*, abs/1810.02244.

[Murphy et al., 2019] Murphy, R. L., Srinivasan, B., Rao, V., and Ribeiro, B. (2019). Relational pooling for graph representations.

[Papillon et al., 2023] Papillon, M., Sanborn, S., Hajij, M., and Miolane, N. (2023). Architectures of topological deep learning: A survey on topological neural networks.

[Ramakrishnan et al., 2014] Ramakrishnan, R., Dral, P., Rupp, M., and von Lilienfeld, A. (2014). Quantum chemistry structures and properties of 134 kilo molecules. *Scientific Data*, 1.

[Satorras et al., 2021] Satorras, V. G., Hoogeboom, E., and Welling, M. (2021). E (n) equivariant graph neural networks. In *International conference on machine learning*, pages 9323–9332. PMLR.

[Sperduti, 1993] Sperduti, A. (1993). Encoding labeled graphs by labeling raam. In Cowan, J., Tesauro, G., and Alspector, J., editors, *Advances in Neural Information Processing Systems*, volume 6. Morgan-Kaufmann.

[Srinivasan and Ribeiro, 2019] Srinivasan, B. and Ribeiro, B. (2019). On the equivalence between node embeddings and structural graph representations. *CoRR*, abs/1910.00452.

[Tailor et al., 2022] Tailor, S. A., Opolka, F., Lio, P., and Lane, N. D. (2022). Adaptive filters for low-latency and memory-efficient graph neural networks. In *International Conference on Learning Representations*.

[Topping et al., 2022] Topping, J., Giovanni, F. D., Chamberlain, B. P., Dong, X., and Bronstein, M. M. (2022). Understanding over-squashing and bottlenecks on graphs via curvature.

[Vaswani et al., 2017] Vaswani, A., Shazeer, N., Parmar, N., Uszkoreit, J., Jones, L., Gomez, A. N., Kaiser, L., and Polosukhin, I. (2017). Attention is all you need. *CoRR*, abs/1706.03762.

[Veličković et al., 2017] Veličković, P., Cucurull, G., Casanova, A., Romero, A., Lio, P., and Bengio, Y. (2017). Graph attention networks. *arXiv preprint arXiv:1710.10903*.

[Wang et al., 2022] Wang, H., Yin, H., Zhang, M., and Li, P. (2022). Equivariant and stable positional encoding for more powerful graph neural networks.

[Weisfeiler and Leman, 1968] Weisfeiler, B. and Leman, A. (1968). The reduction of a graph to canonical form and the algebra which appears therein. *nti, Series*, 2(9):12–16.

[Wu et al., 2018] Wu, Z., Ramsundar, B., Feinberg, E., Gomes, J., Geniesse, C., Pappu, A. S., Leswing, K., and Pande, V. (2018). Moleculenet: a benchmark for molecular machine learning. *Chem. Sci.*, 9:513–530.

[Xu et al., 2018] Xu, K., Hu, W., Leskovec, J., and Jegelka, S. (2018). How powerful are graph neural networks? *CoRR*, abs/1810.00826.

[Ying et al., 2018] Ying, R., He, R., Chen, K., Eksombatchai, P., Hamilton, W. L., and Leskovec, J. (2018). Graph convolutional neural networks for web-scale recommender systems. *CoRR*, abs/1806.01973.

[You et al., 2019] You, J., Ying, R., and Leskovec, J. (2019). Position-aware graph neural networks.

A Random Walk Positional Encoding

The choice of the initial Positional Encoding is critical for introducing topological information into the node representations. Integrating structural and positional encodings enhances the depiction of the graph, resulting in more intricate node embeddings. This, in turn, leads to improved performance in tasks such as node classification, link prediction, and graph generation. Due to the sign flips of Laplacian eigenvector-based PE, [Dwivedi et al., 2021] proposed a Random Walk Positional Encoding scheme (RWPE). The encodings produced with this method carry significant descriptive power when considering graph topology, as they can effectively capture the graph's diffusion characteristics [Topping et al., 2022]. The authors additionally discuss the assumption that RWPE offers a distinctive representation for each node, given that every node possesses a unique topological neighbourhood within a sufficiently large range of k hops.

To further examine the inner workings of RWPE, we provide two samples from the QM9 dataset in Figures 1 and 2, where the first graph has unique RWPE features, while the latter has partially unique features (75 % unique). The plots display a different colour for each unique encoding attributed by RWPE. After some contemplation, one can observe from Figure 1a and 1a, that nodes with the same attributed colour are isomorphic in the graph, i.e. for $k \geq 7$, the nodes have the same k-step neighbourhood.

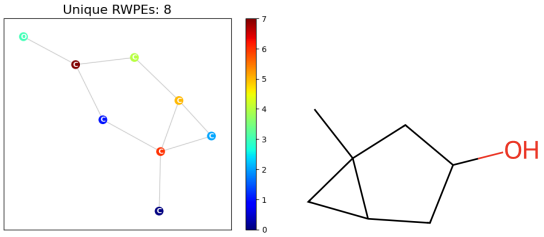

(a) Molecule graph coloured based on RWPE vectors 8/8 unique RWPE

(b) Molecule visualization given SMILES information

Figure 1: Sample molecule graph from the QM9 dataset, alongside the visualization of the corresponding molecule. Index of molecule: **8150**

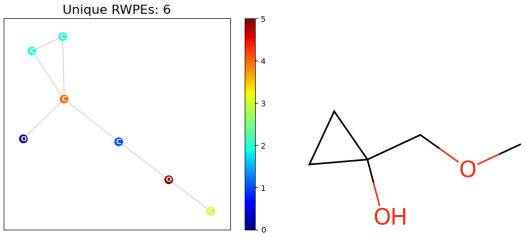

(a) Molecule graph coloured based on RWPE vectors. 6/8 unique RWPE

(b) Molecule visualization given SMILES information

Figure 2: Sample molecule graph from the QM9 dataset, alongside the visualization of the corresponding molecule. Index of molecule: **1755**